Tempo and Mode: Evidence on a Protracted Split From a Dense Fossil Record

Yuri Kimura[1,2,3†], Lawrence J. Flynn[4*†] and Louis L. Jacobs[5†]

[1] National Museum of Nature and Science, Tsukuba, Japan, [2] Department of Geology and Paleontology, National Museum of Nature and Science, Tsukuba, Japan, [3] Institut Català de Paleontologia Miquel Crusafont, ICTA-ICP, Edifici Z. Carrer de les Columnes, s/n., Campus de la Universitat Autònoma de Barcelona, Barcelona, Spain, [4] Department of Human Evolutionary Biology, Harvard University, Cambridge, MA, United States, [5] Roy M. Huffington Department of Earth Sciences, Southern Methodist University, Dallas, TX, United States

Fossil records generally inform paleobiologists about extinct taxa and rates of evolution measured at the scale of millions of years. Good records that are densely sampled through time can reveal species level details such as longevity in local sections. Yet fossil data normally do not address details of lineage microevolution because the density through time of lineage sampling is insufficient to perceive patterns at a precision finer than 10^6 years in most cases. This study concerns details of a splitting event in the evolution of murine rodents, an event for which multiple fossil samples dated to a precision of 10^5 years fortuitously document the tempo and mode of origin of sister species, the stems of two extant tribes of mice. Evolution of early Murinae in the northern part of the biogeographically restricted Indian subcontinent between 11.6 and 10.5 Ma involved cladogenesis of two crown taxa, the extant tribes Murini and Arvicanthini. Large samples of fossil rodent teeth document their divergence from a common morphological pool. Definitive basal Murini and Arvicanthini at 10.5 Ma are similar in size and differ by subtle features of the dentition. Those features occur sporadically in the common pool of older fossil teeth at 11.2, 11.4, and 11.6 Ma as inconsistent polymorphisms. Interpreted as a single lineage in the 11.6–11.2 Ma interval, variability of this abundant murine incorporated the roots of the two crown tribes. The pattern through time suggests morphological stasis for several hundred thousand years prior to splitting. This special case informs us on one example of evolution and shows that the tempo of splitting evolution in some cases may be measured in hundreds of thousands of years, followed by stasis once daughter species have differentiated morphologically.

Keywords: speciation, evolution, Murinae, Miocene, Siwaliks, morphology

INTRODUCTION

Gould (1985) and Reznick and Ricklefs (2009) discussed the importance of the fossil record for evolutionary biology in unveiling major events, especially those under the category of macroevolution. Generally, paleontology does not address details on how evolution proceeds at the population level because relevant data are not sampled densely enough in space and time. In special circumstances, however, the fossil record may be detailed enough to address aspects of evolution

that lie between macro- and microevolution, such as species longevity, changes in abundance, and rates of morphological change. The potential for approaching microevolutionary patterns through the fossil record is great for muroid rodents in cases where stratigraphy and dating are well resolved, and multiple large samples of individuals are available.

Resolution of muroid rodent phylogenetics has had a quantum advance with the application of mitochondrial and nuclear genetic analyses. Steppan and Schenk (2017) resolved a massive amount of data to develop a well-supported hypothesis on relationships of over 900 species. This and previous works (e.g., Lecompte et al., 2008) distinguished major clades of muroids at the family, subfamily, and tribe levels, including tribes Arvicanthini and Murini, both of which have fossil members in South Asia.

Here we set out to interpret a unique fossil record for its relevance to a splitting event that marked the origin of the extant murine rodent tribes Arvicanthini and Murini. Sediments from the Siwalik Group of Pakistan yield a well dated and resolved series of fossil mouse assemblages. We have developed the alpha taxonomy of these species in a series of papers (Jacobs, 1977, 1978; Cheema et al., 2000; Kimura et al., 2015, 2017) and specified the timing of morphological divergence and the emergence of features involved in that divergence (Kimura et al., 2013a,b; Flynn et al., 2020). Early late Miocene Siwalik species assigned to the stem genera *Karnimata* and *Progonomys*, respectively, fortuitously capture the rise of distinctive morphological features that by 10.5–10 million years ago (Ma) characterize dentitions of members of the tribes Arvicanthini and Murini. These features occur in fossil samples from the same geographic area before 11 Ma (Flynn et al., 2020), but inconsistently so that species level taxonomy at that age is problematic.

We contend that the common origin of the Arvicanthini and Murini was recorded in South Asia in Siwalik fossil samples between 12 and 11 Ma. The distinct morphologies of the tribes expressed clearly in fossil species of *Karnimata* and *Progonomys* dating to 10.5 Ma and younger occur across a mix of individuals in the 11.6–11.2 Ma interval that are otherwise inseparable. These appear to be polymorphisms that were stable for hundreds of thousands of years and later characterized the extant tribes.

Our purpose is to document the simultaneous existence of arvicanthin and murinin morphologies in a series of samples from single localities of early late Miocene age, discuss the relevance of their splitting origin within a refined chronology of mouse evolution, and thereby address the tempo and mode of this special event recorded in the fossil record. We interpret these fossils to represent the common ancestral lineage for the two living mouse tribes. Possibly, they represent individuals of closely related cryptic species that did not differ in any other features preserved in the fossils. In either case the time frame for morphological separation of the two tribes is measured in hundreds of thousands of years.

The significance of understanding the tempo and mode of the specific cladogenic event we are studying is that it provides a more confident and precise date for an evolutionary divergence that is relevant for calibrating the molecular phylogeny of essentially every living species of one of the most diverse and speciose groups of mammals in existence, the true mice or Murinae. This group is native to the Old World, including Africa, Australia, and Pacific islands, and global as commensals. It contains the laboratory mouse (*Mus*) and laboratory rat (*Rattus*), long the subject of innumerable studies (da Costa et al., 2019), the former with more than forty living wild species (Suzuki, 2020) and the latter with a confusingly large number of cryptic species (Pages et al., 2010; Rowe et al., 2011). Because fossil murines are known mainly from isolated teeth, the spectrum of morphological characters is limited, which restricts the application of standard morphology-based cladistic analysis. However, the backbone provided by molecular phylogenies of the vast number of living species allows fossil mice to be related confidently.
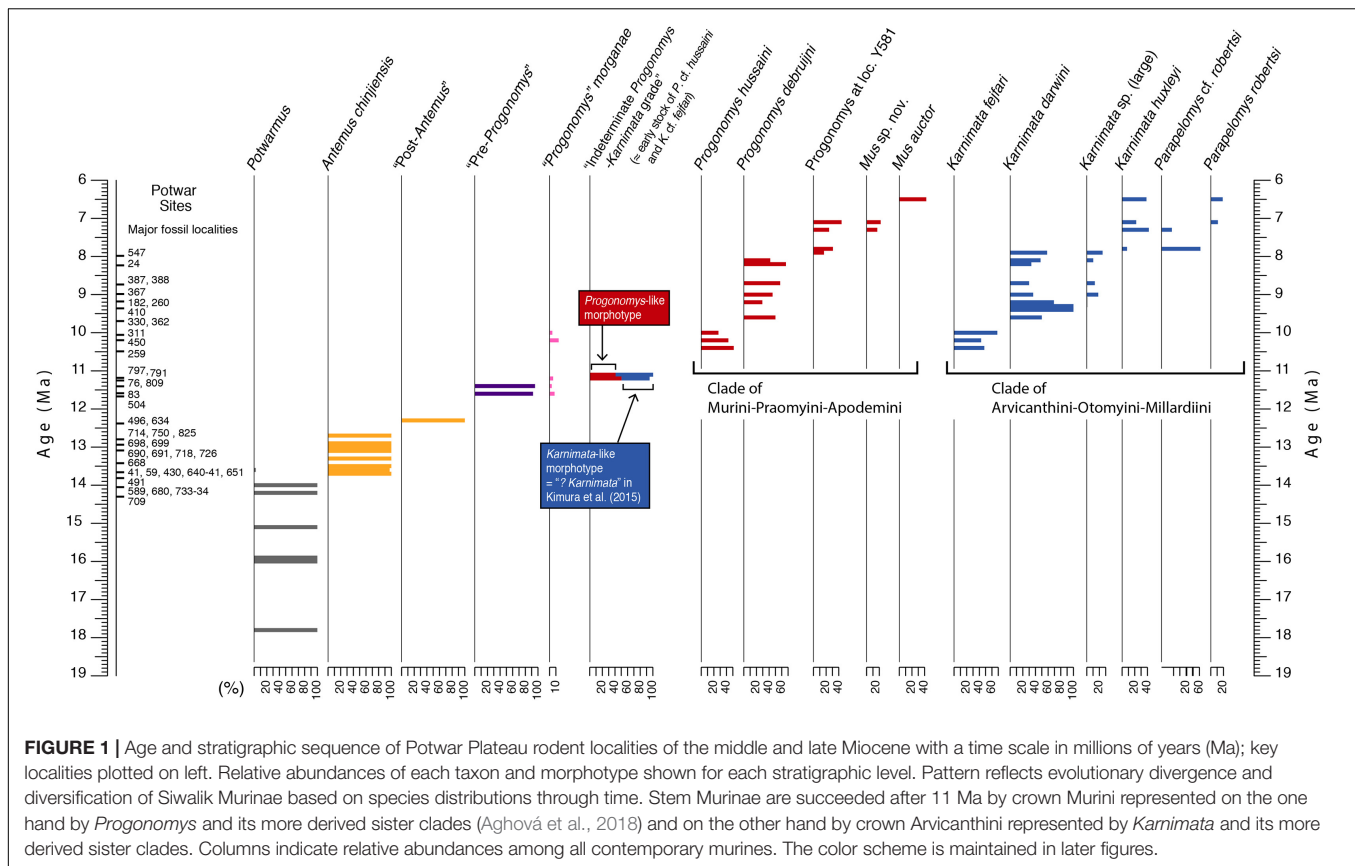
The fossil mice from Pakistan have long been recognized as relevant to calibrating molecular evolutionary hypotheses (Jacobs and Pilbeam, 1980; Jacobs and Flynn, 2005), but earlier studies have been much improved upon by more comprehensive work (e.g., Kimura et al., 2015; Aghová et al., 2018) and the addition of newly studied fossil samples (e.g., Kimura et al., 2017). Divergence dates from Pakistan have been useful in molecular sequence studies applied to biogeography, ecology, and evolutionary patterns (e.g., Rowe et al., 2016, 2019; Bryja et al., 2017), as well as studies of pathogens and genetic mechanisms (e.g., Casola, 2018; Ma et al., 2018), and many other topics. This study contributes by providing a more explicit description of a fossil-based cladogenic event in a precise chronological framework.

MATERIALS AND METHODS

The source of the fossil data is a biostratigraphy of successive rodent sites from the Miocene formations of the Siwalik Group of South Asia. Here we focus on Miocene age sites that are dated 12.5–10 Ma. Each site produces a sample of isolated rodent teeth concentrated most likely by avian predators of the time. Sites contain remains of individuals that died (and are time-averaged) over a decadal to centennial scale. The fossil rodent fauna is represented by squirrels, primitive burrowing rats, hamsters, gerbils, gundis, dormice, and dominant true mice. The series of sites that captures the cladogenic event spans at least 400,000 years from 11.6 to 11.2 Ma. Fossil sites are concentrated in a relatively small area of 200 km^2 near Chinji and Nagri villages on the Potwar Plateau of northern Pakistan (area B in Barry et al., 2002: their Figure 1).

Geology

The Potwar Plateau in northern Pakistan presents an extraordinarily continuous record of Siwalik sediments shed from deformed highlands to the north, the present day mountain ranges bordering the Tibetan Plateau. Drainages carrying detritus southward continue to the present day as components of the mighty Indus River system. The highlands, principally related to the Himalayan and Hindu Kush mountain ranges, have been uplifted continuously throughout the Cenozoic Era by the tectonic forces that thrust the Indian Plate northward under the southern margin of Asia. Currently at 33° North

FIGURE 1 | Age and stratigraphic sequence of Potwar Plateau rodent localities of the middle and late Miocene with a time scale in millions of years (Ma); key localities plotted on left. Relative abundances of each taxon and morphotype shown for each stratigraphic level. Pattern reflects evolutionary divergence and diversification of Siwalik Murinae based on species distributions through time. Stem Murinae are succeeded after 11 Ma by crown Murini represented on the one hand by *Progonomys* and its more derived sister clades (Aghová et al., 2018) and on the other hand by crown Arvicanthini represented by *Karnimata* and its more derived sister clades. Columns indicate relative abundances among all contemporary murines. The color scheme is maintained in later figures.

latitude, the area has moved northward with the Indian plate by about 4° since 11 Ma (Tauxe and Opdyke, 1982). Erosional detritus carried southward and accumulating on pre-Indus floodplains (over 3000 m thick on the Potwar Plateau; Tauxe and Opdyke, 1982) comprise layers of rock of varied lithology, formations of the Siwalik Group. The layers of rock of most interest here, mainly Miocene in age, occur in a broad belt across Indo-Pakistan and as exposed on the Potwar Plateau are ~18–6 million years old (18–6 Ma). The Siwaliks are important for evolutionary biology because the sediments entomb rich samples of the vertebrate biota that populated the region through the Miocene. Fossil bones and teeth are preserved at many levels in the sequence, with the potential that remains of populations in single lineages can be sequentially sampled through time.

The dating of terrestrial fossils through magnetic polarity stratigraphy began in the early 1970's. At that time a consortium of universities began paleontological, stratigraphic, and paleomagnetic studies on the Potwar Plateau because of its fossil abundance known since the 19th Century, its very long fossiliferous stratigraphic section related to the uplift of the Himalaya, and as a focus to develop and validate magnetic polarity stratigraphy in developing a global polarity timescale. From those beginnings, the tradition of precise dating applied to terrestrial paleontology, evolution, and paleoecological studies in the Siwaliks has continued (Keller et al., 1977; Tauxe and Opdyke, 1982; Johnson et al., 1985).

This analysis crucially depends on dated fossil sites with resolution up to 100,000 year precision (see Barry et al., 2002). The dating method involves careful stratigraphic correlation of fossil sites to a master stratigraphic section, in which the paleomagnetic properties of successive samples of rock throughout the stratigraphic sequence build a composite magnetostratigraphy for the Siwaliks. Due to the completeness of the Potwar record, the magnetostratigraphy can be matched to the dated global geomagnetic polarity time scale, yielding age estimates for the rocks (Barry et al., 2013). Estimates are not direct dates, but the dates are relative to one another and distinguishable at a scale of 10^5 years. Because Siwalik strata are generally well exposed, individual fossil localities can be dated in this fashion. This method is widely applied globally (e.g., Garcés et al., 2003; Tedford et al., 2013; Van Dam et al., 2014; García-Paredes et al., 2016).

Siwalik Rodent Fossils

Small mammal fossils accumulated under special conditions at a number of Potwar localities. They are dominantly dental remains presumably accumulated by raptors (mostly owls) in riparian settings. Such conditions did not occur everywhere, so fossil sites are not uniformly distributed through the composite geological section (**Figure 1**)–but they occur densely enough in time to sample details of lineage evolution. Fossils were recovered by wet screening large quantities of fossiliferous sediment from promising localities that usually showed small bone fragments

Age (Ma)	Locality Number	Total Rodent Fossils	Murine Fossils
10.1	Y311	283	205
10.2	Y450	91	41
10.5	Y259	607	395
11.2	Y797	321	108
11.2	Y791	67	48
11.4	Y076	377	142
11.4	Y809	127	67
11.6	Y083	51	17
11.6	Y504	146	52
12.3	Y634	85	32
12.4	Y496	218	88

on the ground surface. After sieving, the concentrate was sorted
under magnification and isolated teeth were retrieved. Samples
of individual species range from a few to several tens of teeth
per site. For the stratigraphic interval capturing the time of
divergence of major murine groups, **Table 1** shows the ages
of localities, the number of rodent fossils recovered from each,
and the number of those rodents that are murines. With fossils,
more complete is always better than less complete, but our use
of isolated teeth was necessitated because that is the nature
of the samples and is mitigated by the observation that living
murine rodent taxa are commonly characterized by molars (e.g.,
Misonne, 1969).

Morphology

Siwalik fossil teeth recovered by screening represent mostly
rodents, but include hedgehogs, shrews, bats, and a few other
mammals. The most abundant rodents retrieved are murine
mice, and these, like all crown muroids, have only molars in each
quadrant behind the enlarged procumbent incisor. The largest
and best represented of the molars is the first upper molar (M1).
Because it is large (by mouse standards) and relatively complex,
this tooth locus presents diagnostic characters and is the most
informative of the molars for systematic study. In some cases, the
first lower molar (m1) is also useful.

Middle Miocene fossils represent stem murines, but exhibit
the apomorphic characteristics of the subfamily, namely extra
cusps in M1 and a twinned anteroconid plus labial cingulum
in m1 (**Figure 2**). These features are derived, absent in muroid
outgroups. The extra cusps in M1 (anterostyle and enterostyle
behind it) are lingual in position and constitute, with neighboring
cusps, transverse sectorial chevrons. In middle Miocene taxa,
the chevrons are poorly developed: most *Potwarmus* (bottom of
Figure 1) lack the anterostyle, and in *Antemus* the enterostyle
is unconnected with its chevron. Jacobs et al. (1989) described
the considerable morphological variation in *Antemus* M1 for a
large sample from locality Y491 (13.8 Ma). Toward the end of
the middle Miocene (12.3 Ma) the early murine lineage, by then
advanced over *Antemus*, exhibited full chevrons on M1, but with
low ridges weakly connecting neighboring cusps. In none of these
samples do we observe definitive features of crown murine tribes.
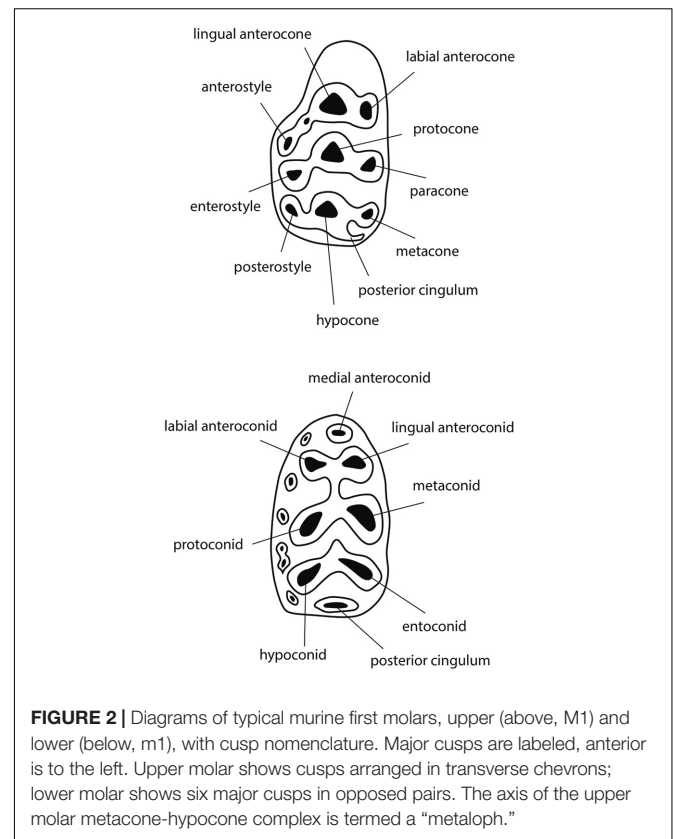
FIGURE 2 | Diagrams of typical murine first molars, upper (above, M1) and
lower (below, m1), with cusp nomenclature. Major cusps are labeled, anterior
is to the left. Upper molar shows cusps arranged in transverse chevrons;
lower molar shows six major cusps in opposed pairs. The axis of the upper
molar metacone-hypocone complex is termed a "metaloph."

Beginning with samples at 11.6 Ma, the debut of the
late Miocene, we observe sporadic occurrence of advanced
M1 features (as below) that characterize crown mouse
tribes. Yet these traits occur in samples of teeth that are
otherwise homogeneous. Characteristic features of Murini and
Arvicanthini appear to be randomly distributed among the
specimens. These mouse teeth represent either a single lineage
with considerable variation, or two lineages that are cryptic as far
as fossil teeth are concerned.

Murini

The key feature of the M1 that characterizes the Murini
concerns the anterostyle (Jacobs, 1978). This lingual cusp
is associated with the first chevron. In Murini the cusp
is shifted posteriorly, its crest running anterolabially to
the double anterocone. The anterior part of the M1 is
therefore transversely narrow. In addition to its posterior
position, the anterostyle is not a circular cusp, but
relatively laterally compressed. Molar cusps are distinctly
inclined posteriorly.

This combination of features appears in some teeth as
a variation in fossil samples of 11.6–11.2 Ma. By 10.5–
10.1 Ma, it is stable. Samples of that age and younger are
readily assigned to the genus *Progonomys*. By the end of the
Miocene, the derivative living genus *Mus* shows a strongly
shifted anterostyle, a narrow anterior shelf surmounted by
the double anterocone, and a reduced posterior cingulum
(Jacobs, 1978).

Arvicanthini

This group conserved the primitive anterostyle position, not strongly repositioned posterolingual to the double anterocone. However, arvicanthins developed progressively a separately derived feature; this concerns the metacone cusp (Kimura et al., 2015). A large metacone that is posteriorly inclined, similar to the paracone, is a primitive condition for mice. The posterior inclination is most obvious in lateral view. Arvicanthins progressively fix a derived condition of the metacone, which is vertical and diminished in size. Most specimens older than 11 Ma show the primitive metacone condition, but some have a modified metacone, smaller than the paracone. By 9.2 Ma, approximately 25% of *Karnimata darwini* show the fully transformed metacone. Progressive development of the derived metacone in the *Karnimata* lineage without similar change in the posterostyle, led Kimura et al. (2015) to recognize that the genus represents a stem in the Arvicanthini-Otomyini-Millardiini clade.

Relative Abundances of Siwalik Murines

Temporal change in the relative abundances of the major components of the Siwalik murine rodents in **Figure 1** is based on the Harvard University-Geological Survey of Pakistan database (e.g., Barry et al., 2013), which is continuously updated. Although the master database includes fossils representing all tooth positions, we analyzed a subset (extracted December, 2020) of only upper first molars (M1) for those taxa with total number of specimens of ten or more. Complexity of M1 maximizes precision of taxonomic assignment for that tooth. The relative abundance of M1 was calculated as the number of fossils in a species (taxonomic unit) relative to the total number of murine fossils. The stratigraphic diagrams were generated with 0.1 m.y. (10^5 year) time bins by the *strat.plot* function in the package *rioja* (Juggins, 2020) implemented in R (R Core Team, 2020).

Crown Morphology in Transition

To visualize change through time of dental characters as they were fixed in the *Mus-Arvicanthis* divergence (**Figure 3** and **Tables 2**–**5**), we obtained the measurements of four morphometric traits of M1 from time-ordered and sequential samples: the ratio of the major and minor axes of the anterostyle; the acute angle of the anterostyle relative to the longitudinal tooth axis; the acute angle between a line connecting the protocone-enterocone and the longitudinal tooth axis; and the acute angle of the metaloph (line through the major axis of the metacone) relative to the longitudinal tooth axis. The datasets of Kimura et al. (2013b) are combined with the latter feature, which is newly obtained for this study. Taxonomic assignments of Kimura et al. (2013b) are updated following Kimura et al. (2015, 2016, 2017) and Flynn et al. (2020). Previously, in Kimura et al. (2013b), we calculated the 95% bias-corrected and accelerated bootstrap (BCa) confidence intervals for groups with more than three entries (i.e., taxa in different time slices are treated as separate groups), and only these data are plotted in Figure 9 of Kimura et al. (2013b). In this study, we calculated both 95% bootstrap confidence intervals for groups with more than two entries. The choice of the bootstrap method did not affect our conclusions. In the bootstrap permutation, 9999 replicates were resampled. The bootstrap confidence intervals were calculated in the R package *boot* (Canty and Ripley, 2020) using the *boot.ci* function. All data are plotted in **Figure 3**. Due to updates in taxonomic assignments, the different bootstrap calculation method, and the selection of groups plotted in **Figure 3**, some details differ slightly from that of Kimura et al. (2013b, Figure 9).
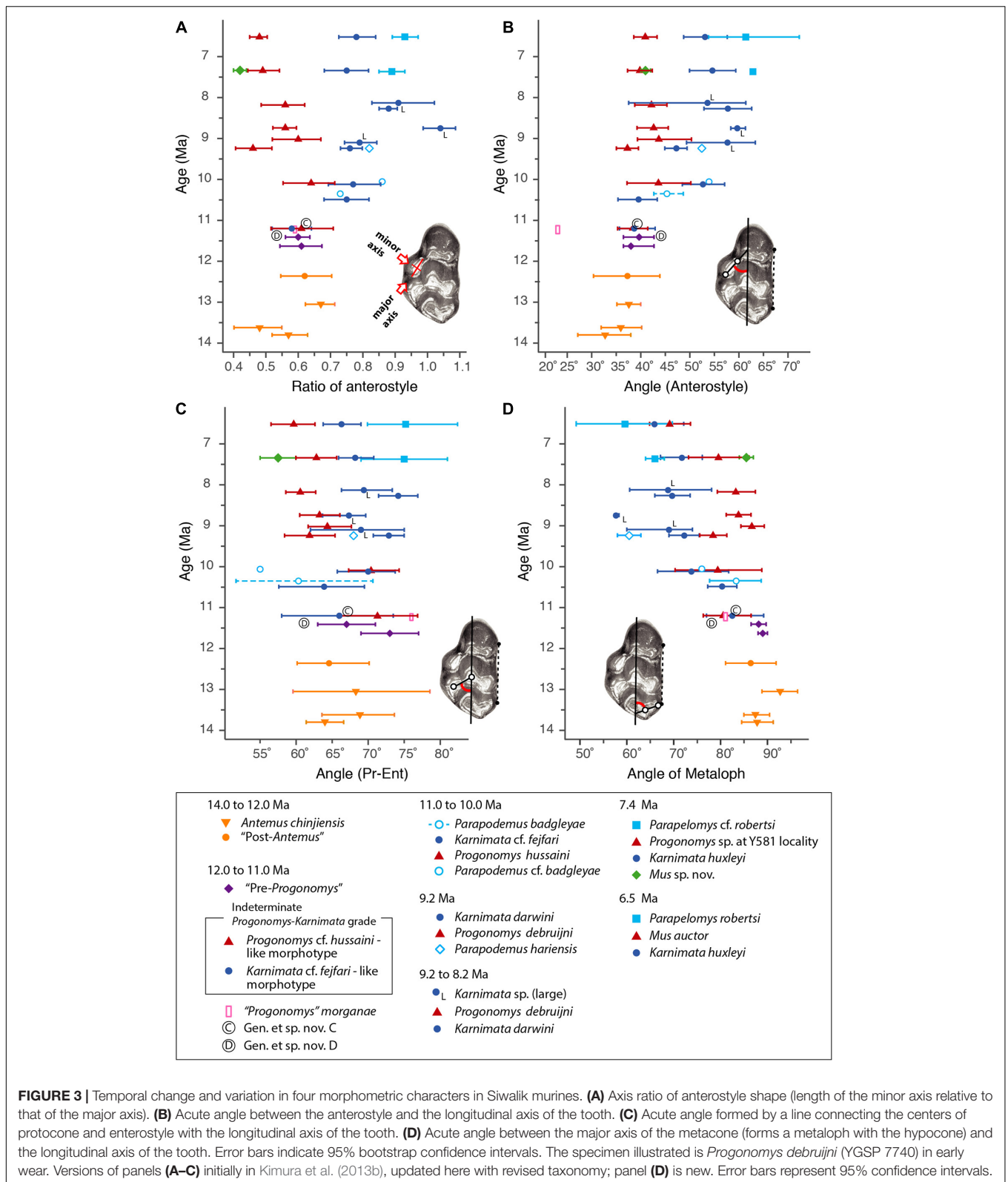
Stratigraphic Age and the Molecular Clock

A time-calibrated tree (discussed below) was generated using "Stratigraphic Tree Analysis for Paleontology" (strap) in R package for proposed relationships of Siwalik murines. We constructed a tree file (.tre) with a single tree as our hypothesis by manually editing tree shape in Mesquite version 3.04 (Maddison and Maddison, 2017) based against an updated review of ranges of Siwalik fossils. For time calibration, first and last appearances were compiled as the lowermost and uppermost stratigraphic occurrences of the taxa. In the R package "strap," the equal scaling method was used in the *DatePhylo* function with a root length (i.e., length of the base of the tree) of 1 million. Although the time-scaling algorithm of the "equal" method is tuned to avoid zero-length branches instead of generating best estimates of divergence times, the model ages of the fossil calibration points are consistent with our previous proposals and molecular estimates (Lecompte et al., 2008; Aghová et al., 2018), and support the proposition that the density of sampled Siwalik fossils may be sufficient to capture transitional morphological changes near divergences.

RESULTS

Previously, we (Flynn et al., 2020) found a good match between the stratigraphic record of clade appearances and the node age estimates from the molecular time tree of Lecompte et al. (2008). Nevertheless, the Siwalik murine record has obtained more detail in recent years from review and analysis of carefully controlled data for over 3600 specimens and therefore the evolution of murines can be traced in more detail. In samples of 9.2 Ma (locality Y182), Jacobs (1978) recognized two clearly separate species, *Progonomys debruijni* and *K. darwini*, now recognized to represent Murini in the former case and Arvicanthini in the latter (**Figure 4**). *P. debruijni* had the murine anterostyle shifted and laterally compressed. All cusps showed posterior inclination and *P. debruijni* was the smaller of the two. The other mouse *K. darwini* was clearly larger with a plesiomorphic anterostyle. Kimura et al. (2013b, 2015) recognized the significance of the morphological distinctions between *Progonomys* and *Karnimata* and distinguished a number of other dental features, including isotopic differences (Kimura et al., 2013a), that set the lineages apart especially after 9 Ma.

In older samples dating to 10.5–10.1 Ma (localities Y259, 450, 311), the murines resembled the 9.2 Ma samples, but represented more primitive species, which Kimura et al. (2017) recognized as *Progonomys hussaini* and *Karnimata fejfari* (**Figure 5**). These earlier representatives of the *Progonomys* and *Karnimata*

FIGURE 3 | Temporal change and variation in four morphometric characters in Siwalik murines. (A) Axis ratio of anterostyle shape (length of the minor axis relative to that of the major axis). (B) Acute angle between the anterostyle and the longitudinal axis of the tooth. (C) Acute angle formed by a line connecting the centers of protocone and enterostyle with the longitudinal axis of the tooth. (D) Acute angle between the major axis of the metacone (forms a metaloph with the hypocone) and the longitudinal axis of the tooth. Error bars indicate 95% bootstrap confidence intervals. The specimen illustrated is *Progonomys debruijni* (YGSP 7740) in early wear. Versions of panels (A–C) initially in Kimura et al. (2013b), updated here with revised taxonomy; panel (D) is new. Error bars represent 95% confidence intervals.

lineages, the stems of Murini and Arvicanthini, were less distinct, showed lower frequency of derived character states, and were much closer in size.

If the older *P. hussaini* and *K. fejfari* were more similar to each other than younger members of these genera (at least in features that could be perceived in the dentition), would

TABLE 2 | Summary statistics for anterostyle ratio in Siwalik murine rodents, corresponding to **Figure 3A**.

Taxonomic Unit	N	Average Age (Ma) GTS2012	Mean	Min	Max	SD	Lower CI basic	Upper CI basic	Lower CI BCa	Upper CI BCa
Karnimata huxleyi	10	6.52	0.78	0.60	0.90	0.09	0.73	0.84	0.72	0.83
Mus auctor	12	6.52	0.48	0.40	0.58	0.05	0.45	0.50	0.45	0.51
Parapelomys robertsi	5	6.52	0.93	0.87	0.98	0.04	0.89	0.97	0.89	0.96
Mus sp. nov.	2	7.34	0.42	0.40	0.44	0.03	0.40	0.44	0.40	0.44
Karnimata huxleyi	20	7.34	0.75	0.45	0.94	0.15	0.68	0.82	0.67	0.81
Progonomys sp. at Y581 locality	11	7.34	0.49	0.37	0.58	0.08	0.44	0.54	0.44	0.53
Parapelomys cf. *robertsi*	2	7.37	0.89	0.85	0.93	0.06	0.85	0.93	0.85	0.93
Karnimata sp. (large)	5	8.13	0.91	0.80	1.02	0.10	0.83	1.02	0.81	1.00
Progonomys debruijni	12	8.18	0.56	0.41	0.87	0.12	0.49	0.62	0.51	0.66
Karnimata darwini	12	8.27	0.88	0.81	0.97	0.05	0.85	0.91	0.85	0.91
Progonomys debruijni	16	8.74	0.56	0.45	0.68	0.07	0.52	0.59	0.52	0.60
Karnimata sp. (large)	3	8.75	1.04	1.00	1.10	0.05	0.99	1.09	1.00	1.10
Progonomys debruijni	3	9.02	0.60	0.53	0.68	0.08	0.52	0.67	0.53	0.68
Karnimata sp. (large)	3	9.10	0.79	0.73	0.83	0.05	0.74	0.84	0.73	0.83
Karnimata darwini	31	9.24	0.76	0.56	0.95	0.10	0.73	0.80	0.73	0.80
Parapodemus hariensis	2	9.24	0.82	0.69	0.95	0.18	0.69	0.95	0.69	0.95
Progonomys debruijni	15	9.24	0.46	0.26	0.61	0.11	0.41	0.52	0.40	0.52
Parapodemys cf. *badgleyae*	1	10.06	0.86	0.86	0.86	NA	NA	NA	NA	NA
Progonomys hussaini	5	10.09	0.64	0.57	0.76	0.09	0.55	0.71	0.58	0.74
Karnimata fejfari	9	10.12	0.77	0.58	0.97	0.12	0.69	0.86	0.69	0.85
Parapodemus badgleyae	3	10.35	0.73	0.73	0.74	0.01	0.73	0.74	0.73	0.74
Karnimata fejfari	9	10.49	0.75	0.62	0.91	0.10	0.68	0.82	0.68	0.82
Gen. et sp. nov. C	1	11.18	0.62	0.62	0.62	NA	NA	NA	NA	NA
"Indeterminate *Progonomys-Karnimata* grade" (*Progonomys*-like morphotype)	7	11.20	0.61	0.46	0.81	0.13	0.52	0.71	0.52	0.72
"Indeterminate *Progonomys-Karnimata* grade" (*Karnimata*-like morphotype)	6	11.20	0.58	0.50	0.68	0.07	0.52	0.64	0.52	0.64
"*Progonomys*" *morganae*	1	11.23	0.59	0.59	0.59	NA	NA	NA	NA	NA
"Pre-*Progonomys*"	21	11.41	0.60	0.49	0.83	0.09	0.56	0.64	0.57	0.65
Gen. et sp. nov. D	1	11.41	0.53	0.53	0.53	NA	NA	NA	NA	NA
"Pre-*Progonomys*"	3	11.63	0.61	0.54	0.67	0.07	0.54	0.67	0.54	0.67
"Post-*Antemus*"	7	12.36	0.62	0.46	0.79	0.11	0.55	0.70	0.55	0.71
Antemus chinjiensis	7	13.05	0.67	0.60	0.75	0.06	0.62	0.71	0.63	0.72
Antemus chinjiensis	14	13.62	0.48	0.31	0.74	0.14	0.40	0.55	0.41	0.56
Antemus chinjiensis	12	13.80	0.57	0.40	0.69	0.10	0.52	0.63	0.51	0.63

CI: 95% confidence interval. BCa: bias-corrected and accelerated bootstrap.
SD: standard deviation.

still older samples (those available to us being 11.6–11.2 Ma) show more subtle differences, or appear to merge? Localities Y797 and Y791, dating to 11.2 Ma, have abundant murines, all about the same size and resembling *Progonomys* and *Karnimata* (plus a few teeth representing small "*Progonomys*" *morganae* and two unnamed mice; Flynn et al., 2020). Most individual specimens appear comparable to *P. hussaini* and *K. fejfari*, but the collections, taken as biological samples, do not sort readily into more than one species. These fossils were considered a single population also in model-based Bayesian cluster analysis

TABLE 3 | Summary statistics for anterostyle angle in Siwalik murine rodents, corresponding to **Figure 3B**.

Taxonomic Unit	N	Average Age (Ma) GTS2012	Mean	Min	Max	SD	Lower CI basic	Upper CI basic	Lower CI BCa	Upper CI BCa
Karnimata huxleyi	10	6.52	53	43	62	7.0	48.7	57.6	48.4	57.3
Mus auctor	12	6.52	41	34	49	4.1	38.6	43.3	38.5	43.2
Parapelomys robertsi	5	6.52	61	50	70	10.0	53.8	72.3	50.3	69.0
Mus sp. nov.	2	7.34	41	40	42	1.4	40.0	42.0	40.0	42.0
Karnimata huxleyi	20	7.34	55	37	72	10.6	49.9	59.4	50.0	59.4
Progonomys sp. at Y581 locality	11	7.34	40	34	45	4.3	37.3	42.3	37.3	42.3
Parapelomys cf. *robertsi*	2	7.37	63	54	72	12.7	69.0	81.0	69.0	81.0
Karnimata sp. (large)	5	8.13	54	45	81	15.4	37.5	61.4	46.3	81.0
Progonomys debruijni	12	8.18	42	34	53	5.7	38.8	45.3	39.2	45.8
Karnimata darwini	12	8.27	58	40	73	8.5	52.9	62.6	52.7	62.4
Progonomys debruijni	16	8.74	43	32	57	6.5	39.3	45.6	39.8	46.2
Karnimata sp. (large)	3	8.75	60	58	61	1.5	58.3	61.3	58.0	61.0
Progonomys debruijni	3	9.02	44	37	48	5.9	39.3	50.3	37.0	48.0
Karnimata sp. (large)	3	9.10	58	52	66	7.4	49.3	63.3	52.0	66.0
Karnimata darwini	31	9.24	47	40	64	6.4	44.9	49.4	45.2	49.8
Parapodemus hariensis	2	9.24	53	45	60	10.6	45.0	60.0	45.0	60.0
Progonomys debruijni	15	9.24	37	31	45	4.5	35.0	39.5	35.1	39.6
Parapodemys cf. *badgleyae*	1	10.06	54	54	54	NA	NA	NA	NA	NA
Progonomys hussaini	5	10.09	44	36	53	6.9	37.2	50.2	37.0	50.0
Karnimata fejfari	9	10.12	53	40	62	6.6	48.5	57.1	47.6	56.5
Parapodemus badgleyae	3	10.35	45	42	48	3.1	42.7	48.7	42.0	48.0
Karnimata fejfari	9	10.49	40	31	51	6.0	35.4	43.4	36.1	44.4
Gen. et sp. nov. C	1	11.18	39	39	39	NA	NA	NA	NA	NA
"Indeterminate *Progonomys-Karnimata* grade" (*Progonomys*-like morphotype)	7	11.20	38	31	43	4.1	35.3	41.4	34.2	40.8
"Indeterminate *Progonomys-Karnimata* grade" (*Karnimata*-like morphotype)	6	11.20	39	30	43	4.6	35.7	42.9	31.8	41.0
"Progonomys" morganae	1	11.23	23	23	23	NA	NA	NA	NA	NA
"Pre-*Progonomys*"	21	11.41	40	28	54	7.3	36.5	42.7	36.7	43.0
Gen. et sp. nov. D	1	11.41	44	44	44	NA	NA	NA	NA	NA
"Pre-*Progonomys*"	3	11.63	38	38	38	0.0	36.5	42.7	36.7	43.0
"Post-*Antemus*"	7	12.36	37	26	51	8.9	30.4	43.9	31.0	44.6
Antemus chinjiensis	7	13.05	38	33	43	3.3	35.1	40.0	35.2	40.2
Antemus chinjiensis	14	13.62	36	22	50	7.9	31.9	40.2	31.4	39.7
Antemus chinjiensis	12	13.80	33	21	50	9.5	27.2	38.0	27.7	38.6

CI: 95% confidence interval. BCa: bias-corrected and accelerated bootstrap.
SD: standard deviation.

(Kimura et al., 2016). Some M1's have the murinin (*Progonomys*-like) morphology and some present the arvicanthin morphology (**Figures 1, 3, 6**). The array of morphologies observed among the M1 is not bimodal–there are intermediates. Further, other molars in the dentition (m1, second and third molars) comprise samples that show no consistent differentiation and no pattern for taxonomic association with M1. For the 11.2 Ma samples Flynn et al. (2020) could not defend two species and opted for an informal designation of "indeterminate *Progonomys–Karnimata* grade." There is no record of *P. hussaini* and *K. fejfari* on

TABLE 4 | Summary statistics for angle formed by the protocone and enterostyle in Siwalik murine rodents, corresponding to **Figure 3C**.

Taxonomic Unit	N	Average Age (Ma) GTS2012	Mean	Min	Max	SD	Lower CI basic	Upper CI basic	Lower CI BCa	Upper CI BCa
Karnimata huxleyi	10	6.52	66	60	72	4.2	63.8	69.0	63.5	68.7
Mus auctor	12	6.52	60	52	69	5.3	56.5	62.6	56.8	63.0
Parapelomys robertsi	5	6.52	75	63	81	7.5	69.9	82.4	63.0	80.0
Mus sp. nov.	2	7.34	58	55	60	3.5	55.0	60.0	55.0	60.0
Karnimata huxleyi	20	7.34	68	53	77	5.6	65.9	70.8	65.3	70.2
Progonomys sp. at Y581 locality	11	7.34	63	55	70	4.8	60.0	65.6	60.0	65.8
Parapelomys cf. *robertsi*	2	7.37	75	69	81	8.5	69.0	81.0	69.0	81.0
Karnimata sp. (large)	5	8.13	69	63	73	4.0	66.3	73.3	63.0	72.0
Progonomys debruijni	12	8.18	61	55	66	3.7	58.6	62.7	58.3	62.5
Karnimata darwini	12	8.27	74	67	81	4.8	71.4	76.9	71.4	76.8
Progonomys debruijni	16	8.74	63	55	75	5.7	60.5	66.1	60.4	66.1
Karnimata sp. (large)	3	8.75	67	65	71	3.2	63.7	69.7	65.0	71.0
Progonomys debruijni	3	9.02	64	61	67	3.1	61.7	67.7	61.0	67.0
Karnimata sp. (large)	3	9.10	69	63	76	6.6	62.0	75.0	63.0	76.0
Karnimata darwini	31	9.24	73	59	87	6.0	70.7	75.0	70.8	75.1
Parapodemus hariensis	2	9.24	68	66	70	2.8	66.0	70.0	66.0	70.0
Progonomys debruijni	15	9.24	62	51	75	6.8	58.4	65.4	58.4	65.4
Parapodemys cf. *badgleyae*	1	10.06	55	55	55	NA	NA	NA	NA	NA
Progonomys hussaini	5	10.09	70	64	74	4.0	67.3	74.3	64.0	73.0
Karnimata fejfari	9	10.12	70	61	83	6.2	65.7	73.8	66.6	74.9
Parapodemus badgleyae	3	10.35	60	50	69	9.6	51.7	70.7	50.0	69.0
Karnimata fejfari	9	10.49	64	50	82	8.9	57.6	69.5	58.8	70.8
Gen. et sp. nov. C	1	11.18	67	67	67	NA	NA	NA	NA	NA
"Indeterminate *Progonomys-Karnimata* grade" (*Progonomys*-like morphotype)	7	11.20	71	59	82	7.1	65.9	76.9	65.3	76.3
"Indeterminate *Progonomys-Karnimata* grade" (*Karnimata*-like morphotype)	6	11.20	66	56	80	9.3	58.0	73.5	58.7	74.2
"*Progonomys*" *morganae*	1	11.23	76	76	76	NA	NA	NA	NA	NA
"Pre-*Progonomys*"	21	11.41	67	51	83	9.3	63.0	71.0	62.9	70.9
Gen. et sp. nov. D	1	11.41	61	61	61	NA	NA	NA	NA	NA
"Pre-*Progonomys*"	3	11.63	73	69	77	4.0	69.0	77.0	69.0	75.7
"Post-*Antemus*"	7	12.36	65	53	70	6.6	60.1	70.1	57.4	68.5
Antemus chinjiensis	7	13.05	68	48	84	12.4	59.6	78.6	57.6	76.6
Antemus chinjiensis	14	13.62	69	54	93	9.8	63.6	73.6	64.5	74.7
Antemus chinjiensis	12	13.80	64	57	71	4.5	61.4	66.6	61.3	66.5

CI: 95% confidence interval. BCa: bias-corrected and accelerated bootstrap.
SD: standard deviation.

the Potwar Plateau prior to 10.5 Ma. The roots of distinct *Progonomys* and of *Karnimata* lineages appear to lie in samples captured at 11.2 Ma.

The mice from Y791 and Y797, 11.2 Ma, were very close to the crown murine genera *Progonomys* and *Karnimata* but did

not show one or the other derived morphologies consistently. Morphologies observed from somewhat older localities were yet more variable, but with inconsistently derived morphologies (**Figure 7**). Our field surveys in subjacent strata located fossil localities Y76 and Y809 at 11.4 Ma, and below these (therefore

TABLE 5 | Summary statistics for axis angle through metacone in Siwalik murine rodents, corresponding to **Figure 3D**.

Taxonomic Unit	N	Average Age (Ma) GTS2012	Mean	Min	Max	SD	Lower CI basic	Upper CI basic	Lower CI BCa	Upper CI BCa
Karnimata huxleyi	10	6.52	66	47	81	9.5	60.2	72.1	59.0	71.3
Mus auctor	12	6.52	69	56	80	7.6	64.9	73.6	64.3	73.0
Parapelomys robertsi	5	6.52	60	41	73	12.1	49.2	69.7	46.3	68.1
Mus sp. nov.	2	7.34	86	84	87	2.1	84.0	87.0	84.0	87.0
Karnimata huxleyi	20	7.34	72	59	97	10.4	67.2	76.1	67.8	76.8
Progonomys sp. at Y581 locality	11	7.34	80	64	91	10.8	73.2	86.1	72.9	85.8
Parapelomys cf. *robertsi*	2	7.37	66	64	68	2.8	64.0	68.0	64.0	68.0
Karnimata sp. (large)	5	8.13	69	56	79	9.3	60.6	78.1	58.3	76.3
Progonomys debruijni	12	8.18	83	71	91	7.3	79.3	87.4	78.6	86.9
Karnimata darwini	12	8.27	70	55	80	6.7	66.0	73.5	65.4	73.1
Progonomys debruijni	16	8.74	84	75	91	5.4	81.2	86.5	81.0	86.3
Karnimata sp. (large)	3	8.75	58	57	58	0.6	57.3	58.3	57.0	58.0
Progonomys debruijni	3	9.02	87	84	89	2.5	84.3	89.3	84.0	89.0
Karnimata sp. (large)	3	9.10	69	64	78	7.8	60.0	74.0	64.0	78.0
Karnimata darwini	31	9.24	72	55	89	9.2	69.0	75.4	69.2	75.7
Parapodemus hariensis	2	9.24	61	58	63	3.5	58.0	63.0	58.0	63.0
Progonomys debruijni	15	9.24	78	67	87	5.6	75.6	81.3	75.4	81.2
Parapodemys cf. *badgleyae*	1	10.06	76	76	76	NA	NA	NA	NA	NA
Progonomys hussaini	5	10.09	79	70	90	9.3	70.3	88.8	70.0	88.0
Karnimata fejfari	9	10.12	74	53	91	11.4	66.6	81.7	65.4	80.8
Parapodemus badgleyae	3	10.35	83	78	89	5.5	77.7	88.7	78.0	89.0
Karnimata fejfari	9	10.49	80	74	86	4.7	77.3	83.5	77.0	83.2
Gen. et sp. nov. C	1	11.18	83	83	83	NA	NA	NA	NA	NA
"Indeterminate *Progonomys-Karnimata* grade" (*Progonomys*-like morphotype)	7	11.20	81	66	87	7.0	76.3	86.5	71.3	84.0
"Indeterminate *Progonomys-Karnimata* grade" (*Karnimata*-like morphotype)	6	11.20	83	72	90	7.6	77.0	89.2	74.0	87.7
"Progonomys" morganae	1	11.23	81	81	81	NA	NA	NA	NA	NA
"Pre-*Progonomys*"	21	11.41	88	81	96	3.7	86.5	89.7	86.6	89.8
Gen. et sp. nov. D	1	11.41	78	78	78	NA	NA	NA	NA	NA
"Pre-*Progonomys*"	3	11.63	89	88	90	1.0	88.0	90.0	88.0	89.7
"Post-*Antemus*"	7	12.36	86	78	97	7.0	81.1	91.9	81.0	91.8
Antemus chinjiensis	7	13.05	93	86	100	5.0	88.8	96.4	89.2	96.8
Antemus chinjiensis	14	13.62	87	74	92	5.3	85.0	90.5	83.2	89.5
Antemus chinjiensis	12	13.80	88	76	98	5.9	84.5	91.3	84.0	90.8

CI: 95% confidence interval. BCa: bias-corrected and accelerated bootstrap.
SD: standard deviation.

older) sites Y83 and Y504 at 11.6 Ma. The collections presented a medley of features, some specimens showing a displaced, pinched anterocone, others showing variably inclined cusps. Individual M1 were occasionally reminiscent of *Progonomys* in having the anterostyle displaced backward (**Figure 7C**), but most molars lacked derived conditions of extant mouse tribes. The M1 resembled their "post-*Antemus*" predecessors of 12.3 Ma, many with anterocones not elongated antero-posteriorly, and connections between adjacent cusps generally undeveloped. These "pre-*Progonomys*" mice were basal crown murines (stem species) containing the roots of later tribe-level radiations, but themselves undifferentiated along modern lines.
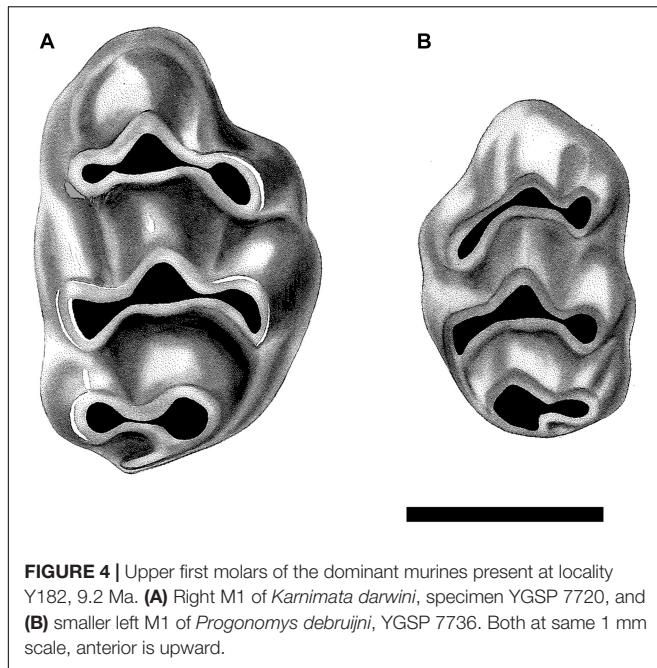
FIGURE 4 | Upper first molars of the dominant murines present at locality Y182, 9.2 Ma. **(A)** Right M1 of *Karnimata darwini*, specimen YGSP 7720, and **(B)** smaller left M1 of *Progonomys debruijni*, YGSP 7736. Both at same 1 mm scale, anterior is upward.
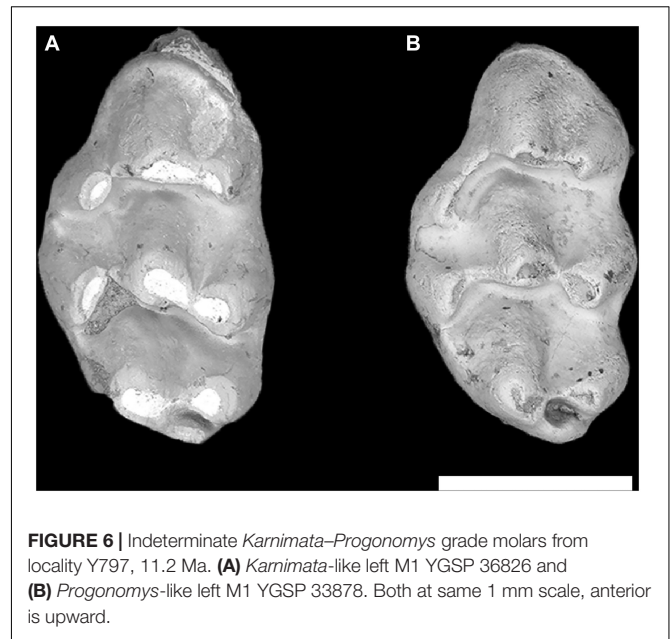

FIGURE 6 | Indeterminate *Karnimata–Progonomys* grade molars from locality Y797, 11.2 Ma. **(A)** *Karnimata*-like left M1 YGSP 36826 and **(B)** *Progonomys*-like left M1 YGSP 33878. Both at same 1 mm scale, anterior is upward.
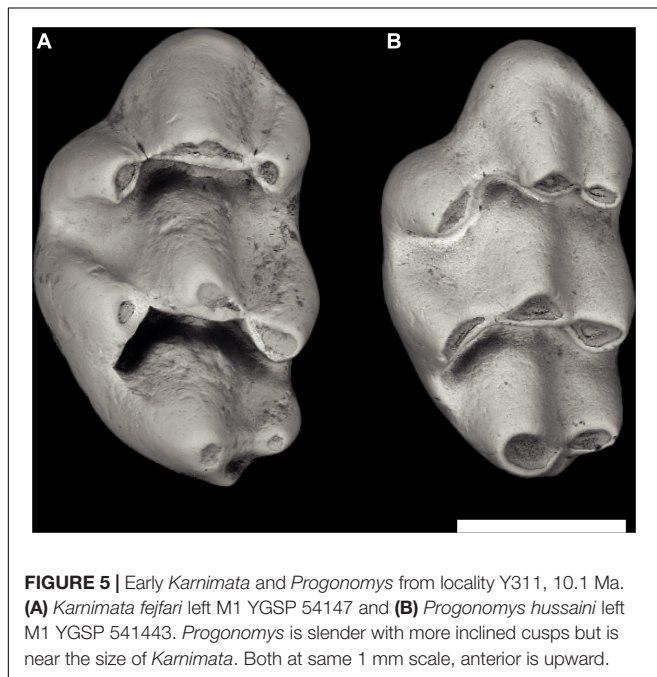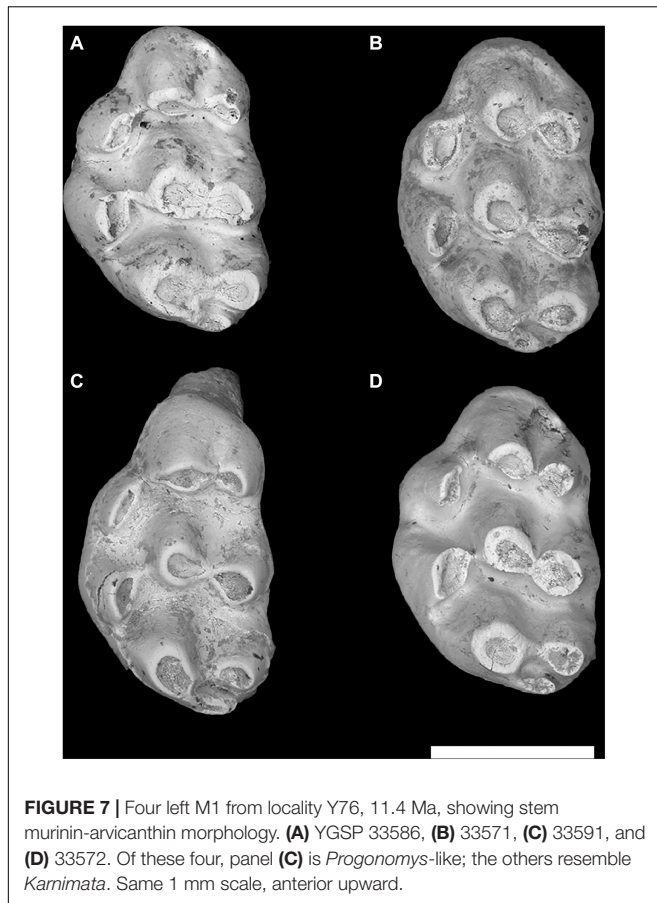

FIGURE 5 | Early *Karnimata* and *Progonomys* from locality Y311, 10.1 Ma. **(A)** *Karnimata fejfari* left M1 YGSP 54147 and **(B)** *Progonomys hussaini* left M1 YGSP 541443. *Progonomys* is slender with more inclined cusps but is near the size of *Karnimata*. Both at same 1 mm scale, anterior is upward.

The documentation of multiple, sequentially progressive transitional samples, whether of mixed cryptic species or of consecutive individually variable species, provides a timescale for this cladistic event and a view of its mode. In either case, the 11 Ma divergence provided by "*strap*"-based stratigraphic age estimation (**Figure 8**) is congruent with the most recent molecular estimates of the Murini-Arvicanthini split provided by Aghová et al. (2018).

DISCUSSION

It is well worth emphasizing the unique set of conditions that allowed this evaluation of tempo and mode in evolution using the fossil record. Siwalik Group rocks or their equivalents span a vast area along the Himalaya front from Pakistan to Myanmar. Correlative fossils from India largely complement and corroborate the Siwalik murine record in Pakistan (Patnaik, 2014, 2020). Older fossils are not relevant to this study because they are phylogenetically distant from the problem; younger fossil taxa are more derived members of Murini and Arvicanthini (e.g., Jacobs, 1978; Musser, 1987; Patnaik et al., 1993, 2018; Kotlia, 2008; Patnaik, 2020). Although fossil murines and other fossil rodents have been known in Europe (Schaub, 1938; Michaux, 1971) and globally for many years, no murine fossil known is older than the oldest murines of Pakistan. Flynn et al. (2020) have discussed this restricted biogeographic setting of the Siwaliks as the "murine cradle."

Moreover, Siwalik murines and other small mammals were linked with the remainder of the fauna as part of a large, evolving ecosystem that responded to global conditions (Barry et al., 1985; Blois and Hadley, 2009; Figueirido et al., 2012) and to more regional abiotic and climatic changes (Flynn and Jacobs, 1982; Badgley et al., 2008; López-Antoñanzas et al., 2015). Stable isotopes have been used to track changes in Siwalik murine diets and tooth morphology has been correlated with dietary changes (Kimura et al., 2013a,b, 2016). These aspects of paleobiology, all of which have a temporal component, reiterate the importance of high-quality geologic dating and dense sampling of fossils in the Siwaliks. Finally, the group of animals being studied, with an enormous modern diversity and broad geographic range, renders the study of their deep roots both multidisciplinary and highly significant.

FIGURE 7 | Four left M1 from locality Y76, 11.4 Ma, showing stem murinin-arvicanthin morphology. **(A)** YGSP 33586, **(B)** 33571, **(C)** 33591, and **(D)** 33572. Of these four, panel **(C)** is *Progonomys*-like; the others resemble *Karnimata*. Same 1 mm scale, anterior upward.

The middle and late Miocene age murine fossil record is rich throughout the Old World, but the oldest fossils of the subfamily are from the early Miocene of South Asia (Flynn et al., 2020). Significant events in early murine evolution appear to be centered in southern Asia, and the best fossil record that captures part of that radiation is being developed in the Siwaliks of the Indian Subcontinent (Jacobs and Downs, 1994; Jacobs and Flynn, 2005; Patnaik, 2014). This exceptional fossil record bears on the origin of two extant tribes, Murini and Arvicanthini. We contend that while the fossil record does not address population microevolution, it is relevant to fine scale evolutionary phenomena between the microevolutionary and macroevolutionary levels.

The Siwalik deposits of the Potwar Plateau contain a record of superposed fossil samples that is continuous and well dated on the scale of 100,000 years especially for the time span discussed here, 14–8 Ma. We have applied this precise biostratigraphy to a special episode in murine evolution. The relative ages of fossils are consistent with the pattern of evolution of crown clades (Lecompte et al., 2008; Aghová et al., 2018; Flynn et al., 2020).

Major morphological features are in this case an insufficient basis for tracing microevolution so we dissected molar crown morphology into distinct, definable traits and traced change
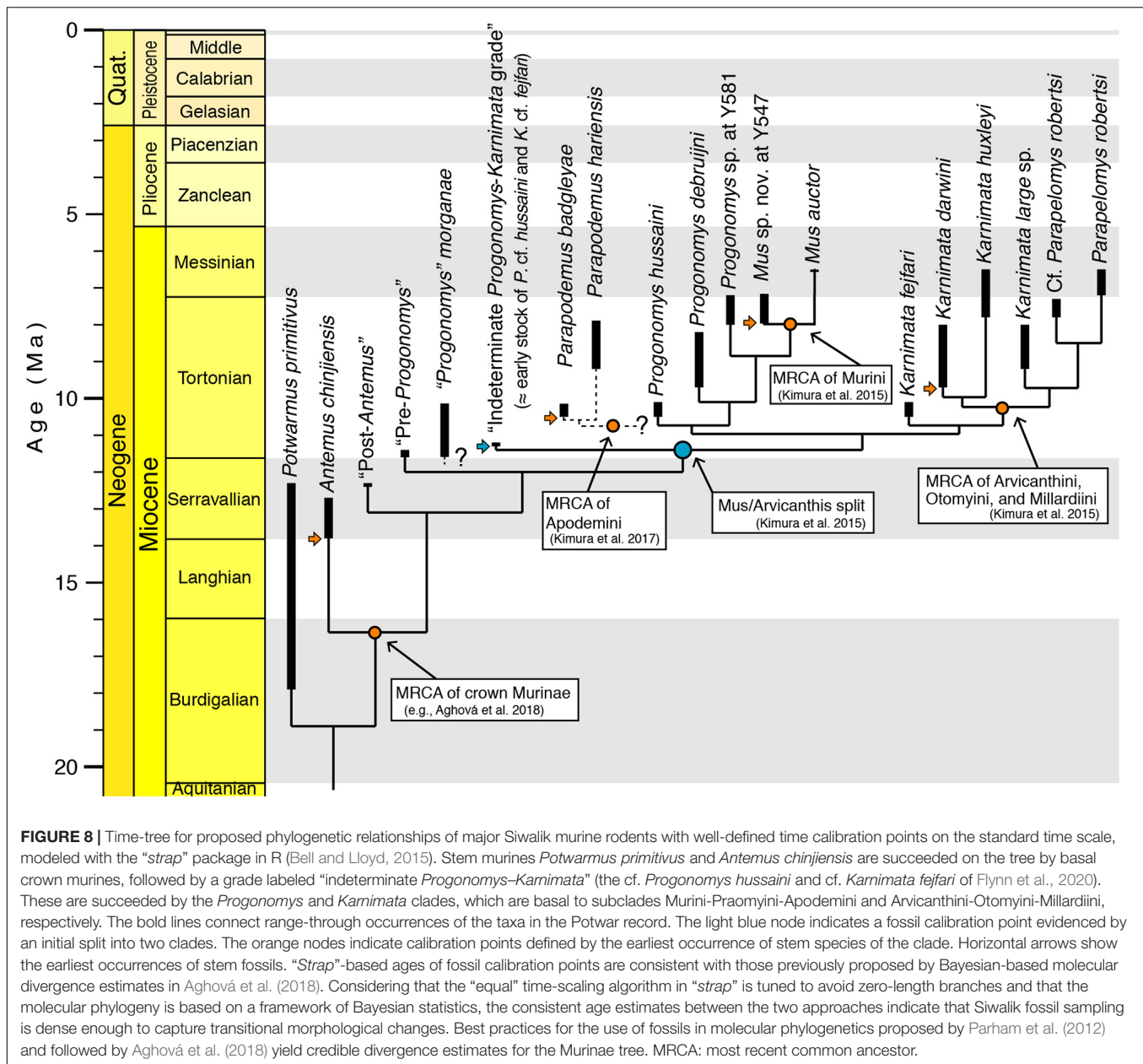
through time (**Figure 3**). We selected four features (see section "Materials and Methods") and quantified change from 14 to 6 Ma. These features show considerable variation until about 11 Ma, when they diverge, slowly at first, as Murini and Arvicanthini (and other minor lineages). We contend that this faithfully reflects growing divergence in morphology consistent with the scenario of a split of the two lineages from a common ancestor, with clear separation by 10.5 Ma.

Fossil samples at 9.2 Ma and younger securely represent early Murini and Arvicanthini in morphological features and dietary preferences (Kimura et al., 2015, 2016). Key species at that age are the distinct *P. debruijni* and *K. darwini*. Predecessor species, *P. hussaini* and *K. fejfari*, occur in rocks one million years older. These species were morphologically closer to each other than their successors were to their contemporaries, but still distinct, and are closer in time to the origins of the tribes. The oldest records of *P. hussaini* and *K. fejfari* are from locality Y259 at 10.5 Ma; they may well have been distinct before that. However, at 11.2 Ma we find that while the species were not yet present, samples are consistent with the hypothetical origin of Murini and Arvicanthini. Fossil samples at 11.2 Ma comprise morphological variants that resemble *Progonomys* and *Karnimata* but appear to represent a single lineage of rodents. The samples do not present a bimodal distribution of shape or size. Hypothetical cryptic species may be a possibility but cannot be distinguished morphologically.

These data speak to the *mode* of evolution in these murines. The split of the modern tribes was incremental. It began in a common pool of morphological variants. Extremes in variation, e.g., the murinin anterostyle, became hallmarks of mice exploiting one part of the range of variation, in contrast to the arvicanthin strategy of retained vertical cusps and broadened molars. Absolute change in M1 morphology is greater in arvicanthins, which later exploited preferentially a C4 diet. Our data suggest such a scenario but are not sufficient to claim that the tribes originated at 11.2 Ma exactly. Indeed, the lineages may have been close, but not yet morphologically distinct at that age in the features we can perceive. The fossils at 11.2 Ma may sample two cryptic species, *Progonomys* and *Karnimata* ancestors.

The Siwalik fossil record also addresses the *tempo* of the origin of Murini and Arvicanthini. Prior to 11.2 Ma, fossil samples show similar variation embracing early murinin and arvicanthin morphology. This suggests a very long interval of time during which basal crown murines experimented with diversification as Murini and Arvicanthini. Hundreds of thousands of years passed before the definitive tribe-equivalent morphologies emerged. Even if *Progonomys* and *Karnimata* had diverged by 11.2 Ma, the completion of their splitting process was protracted over a very long time, at least 400,000 years during this interval.

What may have gone on during these 100,000 years? While the clear separation of crown tribes may be arbitrary within tight limits, it is quite feasible that gene flow, even if limited, continued between their earliest species members for some time after their genetic divergence. The phenomenon of genetic

FIGURE 8 | Time-tree for proposed phylogenetic relationships of major Siwalik murine rodents with well-defined time calibration points on the standard time scale, modeled with the "*strap*" package in R (Bell and Lloyd, 2015). Stem murines *Potwarmus primitivus* and *Antemus chinjiensis* are succeeded on the tree by basal crown murines, followed by a grade labeled "indeterminate *Progonomys–Karnimata*" (the cf. *Progonomys hussaini* and cf. *Karnimata fejfari* of Flynn et al., 2020). These are succeeded by the *Progonomys* and *Karnimata* clades, which are basal to subclades Murini-Praomyini-Apodemini and Arvicanthini-Otomyini-Millardiini, respectively. The bold lines connect range-through occurrences of the taxa in the Potwar record. The light blue node indicates a fossil calibration point evidenced by an initial split into two clades. The orange nodes indicate calibration points defined by the earliest occurrence of stem species of the clade. Horizontal arrows show the earliest occurrences of stem fossils. "Strap"-based ages of fossil calibration points are consistent with those previously proposed by Bayesian-based molecular divergence estimates in Aghová et al. (2018). Considering that the "equal" time-scaling algorithm in "*strap*" is tuned to avoid zero-length branches and that the molecular phylogeny is based on a framework of Bayesian statistics, the consistent age estimates between the two approaches indicate that Siwalik fossil sampling is dense enough to capture transitional morphological changes. Best practices for the use of fossils in molecular phylogenetics proposed by Parham et al. (2012) and followed by Aghová et al. (2018) yield credible divergence estimates for the Murinae tree. MRCA: most recent common ancestor.

introgression within a temporal murine metacommunity over a long interval before complete isolation of daughter species (Presgraves and Yi, 2009) has important implications for interpreting age of lineage splitting and therefore the molecular clock. The timing of cladogenesis as perceived by paleontologists from preserved morphology may post-date significantly a protracted interval of gene exchange at the base of the split. We have been fortunate to be able to view the results of one cladogenic event in detail, the split of Tribes Murini and Arvicanthini. That process may unfold quickly or take hundreds of thousands of years for significant morphological change to accumulate. Judging from our case, morphological change following sporadic genetic divergence may be a significantly protracted process.

DATA AVAILABILITY STATEMENT

The original contributions presented in the study are included in the article/supplementary material, further inquiries can be directed to the corresponding author/s.

AUTHOR CONTRIBUTIONS

All authors contributed equally to this work and each agrees to be accountable for the content of the work. YK developed much of the original comparative data and developed the temporo-stratigraphic analyses. LJ integrated the morphological

and molecular patterns into a coherent whole, and organized specimen imaging. LF applied this special case for the fossil record to current molecular records and revised specimen identifications and locality dating.

FUNDING

ACKNOWLEDGMENTS

REFERENCES

Aghová, T., Kimura, Y., Bryja, J., Dobigny, G., Granjon, L., and Kergoat, G. J. (2018). Fossils know it best: using a new set of fossil calibrations to improve the temporal phylogenetic framework of murid rodents (Rodentia: muridae). *Mol. Phylogenet. Evol.* 128, 98–111. doi: 10.1016/j.ympev.2018.07.017

Badgley, C., Barry, J. C., Morgan, M. E., Nelson, S. V., Behrensmeyer, A. K., Cerling, T. E., et al. (2008). Ecological changes in Miocene mammalian record show impact of prolonged climatic forcing. *Proc. Natl. Acad. Sci. U.S.A.* 105, 12145–12149. doi: 10.1073/pnas.0805592105

Barry, J. C., Behrensmeyer, A. K., Badgley, C. E., Flynn, L. J., Peltonen, H., Cheema, I. U., et al. (2013). "The neogene siwaliks of the potwar plateau, Pakistan," in *Fossil Mammals of Asia: Neogene Biostratigraphy and Chronology*, eds X. Wang, L. J. Flynn, and M. Fortelius (New York, NY: Columbia University Press), 373–398. doi: 10.7312/columbia/9780231150125.003.0015

Barry, J. C., Johnson, N. M., Raza, S. M., and Jacobs, L. L. (1985). Neogene mammalian faunal change in Southern Asia: correlations with climatic, tectonic, and eustatic events. *Geology* 13, 637–640. doi: 10.1130/0091-7613(1985)13<637:nmfcis>2.0.co;2

Barry, J. C., Morgan, M. E., Flynn, L. J., Pilbeam, D., Behrensmeyer, A. K., Raza, S. M., et al. (2002). Faunal and environmental change in the late Miocene Siwaliks of northern Pakistan. *Paleobiol. Memoir.* 28, 1-71.

Bell, M. A., and Lloyd, G. T. (2015). STRAP: an R package for plotting phylogenies against stratigraphy and assessing their stratigraphic congruence. *Palaeontology* 58, 379–389. doi: 10.1111/pala.12142

Blois, J. L., and Hadley, E. A. (2009). Mammalian response to Cenozoic climatic change. *Annu. Rev. Earth Planet. Sci.* 37, 181–208. doi: 10.1146/annurev.earth.031208.100055

Bryja, J., Sumbera, R., Peterhans, J. C. K., Aghová, T., Bryjova, A., Mikula, O., et al. (2017). Evolutionary history of the, thicket rats (genus *Grammomys*) mirrors the evolution of African forests since late Miocene. *J. Biogeogr.* 44, 182–194. doi: 10.1111/jbi.12890

Canty, A., and Ripley, B. D. (2020). *Boot: Bootstrap R (S-Plus) Functions. R Package Version 1.3-25*.

Casola, C. (2018). From de novo to "de Nono": the majority of novel protein coding genes identified with phylostratigraphy are old genes or recent duplicates. *Genome Biol. Evol.* 10, 2906–2918. doi: 10.1093/gbe/evy231

Cheema, I. U., Raza, S. M., Flynn, L. J., Rajpar, A. R., and Tomida, Y. (2000). Miocene small mammals from Jalalpur (District Jhelum) and their biochronologic implications. *Natl. Sci. Mus. Bull.* 26, 57–77. Tokyo,

da Costa, S. M., Rossi, M. I. D., Evangelista, A. A., and Oliveira, G. M. (2019). Origin, phylogeny and natural behavior of mice: what is their influence on welfare during their maintenance in the house facilities? *Amer. J. Biomed. Sci.* 5:AJBSR.MS.ID.000946. doi: 10.34297/AJBSR.2019.05.000946

Figueirido, B., Janis, C. M., Pérez-Claros, J. A., De Renzi, M., and Palmqvist, P. (2012). Cenozoic climate change influences mammalian evolutionary dynamics. *Proc. Natl. Acad. Sci. U.S.A.* 109, 722–727. doi: 10.1073/pnas.1110246108

Flynn, L. J., and Jacobs, L. L. (1982). Effects of changing environments on Siwalik rodent faunas of northern Pakistan. *Palaeogeogr. Palaeoclimatol. Palaeoecol.* 38, 129–139. doi: 10.1016/0031-0182(82)90067-0

Flynn, L. J., Kimura, Y., and Jacobs, L. L. (2020). "The murine cradle," in *Biological Consequences of Plate Tectonics: New Perspectives on Post-Gondwanaland Break-Up*, eds G. V. R. Prasad, and R. Patnaik (Cham: Springer), 347–362.

Garcés, M., Krijgsmann, W., Paláez-Campomanes, P., Álvarez-Sierra, M. A., and Daams, R. (2003). *Hipparion* dispersal in Europe: magnetostratigraphic constraints from the Daroca area (Spain). *Coloq. Paleontol.* 1, 171–178.

García-Paredes, I., Álvarez-Sierra, M. A., van den Hoek Ostende, L. W., Hernández-Ballarin, V., Hordijk, K., López-Guerro, P., et al. (2016). The Aragonian and Vallesian high-resolution micromammal succession from the Calatayud-Montalbán Basin (Aragón, Spain). *C. R. Palevol* 15, 781–789. doi: 10.1016/j.crpv.2015.09.014

Gould, S. J. (1985). The paradox of the first tier: an agenda for paleobiology. *Paleoiology* 11, 2–12. doi: 10.1017/s0094837300011350

Jacobs, L. L. (1977). A new genus of murid rodent from the Miocene of Pakistan and comments on the origin of the Muridae. *Paleobios* 25, 1–11.

Jacobs, L. L. (1978). Fossil rodents (Rhizomyidae and Muridae) from Neogene Siwalik deposits, Pakistan. *Mus. North. Arizona Press Bull.* 52, 1–103.

Jacobs, L. L., and Downs, W. R. (1994). "The evolution of murine rodents in Asia," in *Rodent and Lagomorph Families of Asian Origins and Diversification*, Vol. 8, eds Y. Tomida, C.-k. Li, and T. Setoguchi (Tokyo: National Science Museum Monograph), 149–156.

Jacobs, L. L., and Flynn, L. J. (2005). "Of mice again: the Siwalik rodent record, murine distribution, and molecular clocks," in *Interpreting the Past: Essays on Human, Primate, and Mammal Evolution in Honor of David Pilbeam*: American School of Prehistoric Research Monograph Series 5, eds D. E. Lieberman, R. J. Smith, and J. Kelley (Boston, MA: Brill Academic Publishers, Inc.), 63–80.

Jacobs, L. L., Flynn, L. J., and Downs, W. R. (1989). "Neogene rodents of southern Asia," in *Papers on Fossil Rodents in Honor of Albert Elmer Wood*, Vol. 33, eds C. C. Black, and M. R. Dawson (Los Angeles, CA: Natural History Museum of Los Angeles County), 157–177.

Jacobs, L. L., and Pilbeam, D. (1980). Of mice and men: fossil-based divergence dates and molecular "clocks". *J. Hum. Evol.* 9, 551–555. doi: 10.1016/0047-2484(80)90062-7

Johnson, N. M., Stix, J., Tauxe, L., Cerveney, P. F., and Tahirkheli, R. A. K. (1985). Paleomagnetic chronology, fluvial processes, and tectonic implications of the Siwalik deposits near Chinji Village, Pakistan. *J. Geol.* 93, 27–40. doi: 10.1086/628917

Juggins, S. (2020). *rioja: Analysis of Quaternary Science Data. R Package Version 0.9-26*. Available online at: https://cran.r-project.org/package=rioja (accessed December 15, 2020).

Keller, H. M., Tahirkheli, R. A. K., Mirza, M. A., Johnson, G. D., Johnson, N. M., and Opdyke, N. D. (1977). Magnetic polarity stratigraphy of the Upper Siwalik Deposits, Pabbi Hills, Pakistan. *Earth Planet. Sci. Lett.* 36, 187–201. doi: 10.1016/0012-821x(77)90198-4

Kimura, Y., Flynn, L. J., and Jacobs, L. L. (2016). A palaeontological case study for species delimitation in diverging fossil lineages. *Hist. Biol.* 28, 189–198. doi: 10.1080/08912963.2015.1022175

Kimura, Y., Flynn, L. J., and Jacobs, L. L. (2017). Early late Miocene murine rodents from the upper part of the Nagri Formation, Siwalik Group, Pakistan, with a new fossil calibration point for the Tribe Apodemurini (*Apodemus/Tokudaia*). *Fossil Imprint* 73, 197–212. doi: 10.2478/if-2017-0011

Kimura, Y., Hawkins, M. T. R., McDonough, M. M., Jacobs, L. L., and Flynn, L. J. (2015). Corrected placement of *Mus-Rattus* fossil calibration forces precision in the molecular tree of rodents. *Sci. Rep.* 5:14444. doi: 10.1038/srep 14444

Kimura, Y., Jacobs, L. L., Cerling, T. E., Uno, K. T., Ferguson, K. M., Flynn, L. J., et al. (2013a). Fossil mice and rats show isotopic evidence of niche partitioning and change in dental ecomorphology related to dietary shift in late Miocene of Pakistan. *PLoS One* 8:e69308. doi: 10.1371/journal.pone.0069308

Kimura, Y., Jacobs, L. L., and Flynn, L. J. (2013b). Lineage-specific responses of tooth shape in murine rodents (Murinae, Rodentia) to late Miocene dietary change in the Siwaliks of Pakistan. *PLoS One* 8:e76070. doi: 10.1371/journal. pone.0076070

Kotlia, B. S. (2008). A new species of fossil *Mus* (Rodentia, Muridae) from the Indian Himalaya: evolutionary and phylogenetic implications. *Palaeoworld* 17, 47–56. doi: 10.1016/j.palwor.2007.08.004

Lecompte, E., Aplin, K., Denys, C., Catzeflis, F., Chades, M., and Chevret, P. (2008). Phylogeny and biogeography of African Muridae based on mitochondrial and nuclear gene sequences, with a new tribal classification of the subfamily. *BMC Evol. Biol.* 8:199. doi: 10.1186/1471-2148-8-199

López-Antoñanzas, R., Knoll, F., Wan, S., and Flynn, L. J. (2015). Causal evidence between monsoon and evolution of rhizomyine rodents. *Sci. Rep.* 5:9008. doi: 10.1038/srep09008

Ma, L., Cisse, O. H., and Kovacs, J. A. (2018). A molecular window into the biology and epidemiology of *Pneumocystis* spp. *Clin. Microbiol. Rev.* 31:e00009-18. doi: 10.1128/CMR.00009-18

Maddison, W. P., and Maddison, D. R. (2017). *Mesquite: A Modular System for Evolutionary Analysis. Version 3.04.* Available online at: http://mesquiteproject. org (accessed December 12, 2020).

Michaux, J. (1971). Muridae (Rodentia) neogenes d'Europe Sud-Occidentale: evolution et rapports avec les formes actuelles. *Paleobiol. Continentale* 2, 1–67.

Misonne, X. (1969). *African and Indo-Australian Muridae Evolutionary Trends*: Annales. Sciences Zoologique 8. Tervuren: Musée Royal de l'Afrique Centrale, 1–219.

Musser, G. G. (1987). The occurrence of *Hadromys* (Rodentia: muridae) in early Pleistocene Siwalik strata in northern Pakistan and its bearing on biogeographic affinities between Indian and northeastern African murine faunas. *Am. Mus. Novitates* 2883, 1–36.

Pages, M., Chaval, Y., Herbreteau, V., Waengsothorn, S., Cosson, J.-F., Hugot, J.-P., et al. (2010). Revisiting the taxonomy of the Rattini tribe: a phylogeny-based delimitation of species boundaries. *BMC Evol. Biol.* 10:184. doi: 10.1186/1471-2148-10-184

Parham, J. F., Donoghue, P. C., Bell, C. J., Calway, T. D., Head, J. J., Holroyd, P. A., et al. (2012). Best practices for justifying fossil calibrations. *Syst. Biol.* 61, 346–359.

Patnaik, R. (2014). Phylogeny of Siwalik murine rodents: implications for *Mus-Rattus* divergence time. *J. Palaeontol. Soc. India* 59, 15–28.

Patnaik, R. (2020). "New data on the Siwalik murines, rhizomyines and ctenodactylines (Rodentia) from the Indian subcontinent," in *Biological Consequences of Plate Tectonics: New Perspectives on Post-Gondwanaland Break-Up*, eds G. V. R. Prasad, and R. Patnaik (Cham: Springer), 363–391. doi: 10.1007/978-3-030-49753-8_16

Patnaik, R., Bahadur, M., Sharma, T., and Sahni, A. (1993). A comparative analysis of the molars of *Mus booduga*, *Mus dunni* and fossil *Mus* of the Indian

subcontinent: phylogenetic and palaeobiogeographic implications. *Curr. Sci.* 65, 782–786.

Patnaik, R., Kotla, S. S., Singh, N. P., Singla, A., and Kaur, J. (2018). A new murid rodent assemblage from the Upper Siwaliks, Himachal Pradesh, India: biostratigraphic, phylogenetic and paleobiogeographic implications. *J. Asian Earth Sci.* 162, 93–106. doi: 10.1016/j.jseaes.2017.05.030

Presgraves, D. C., and Yi, S. V. (2009). Doubts about complex speciation between humans and chimpanzees. *Trends Ecol. Evol.* 24, 533–540. doi: 10.1016/j.tree. 2009.04.007

R Core Team (2020). *R: A Language and Environment for Statistical Computing*. Vienna: R. Foundation for Statistical Computing.

Reznick, D. N., and Ricklefs, R. E. (2009). Darwin's bridge between microevolution and macroevolution. *Nature* 457, 837–842. doi: 10.1038/nature 07894

Rowe, K. C., Achmadi, A. S., and Esselstyn, J. A. (2016). Repeated evolution of carnivory among Indo-Australian rodents. *Evolution* 70, 653–665. doi: 10.1111/ evo.12871

Rowe, K. C., Achmadi, A. S., Fabre, P.-H., Schenk, J. J., Steppen, S. J., and Esselstyn, J. A. (2019). Oceanic islands of Wallacea as a source for dispersal and diversification of murine rodents. *J. Biogeogr.* 46, 2752–2768. doi: 10.1111/jbi. 13720

Rowe, K. C., Aplin, K. P., Baverstock, P. R., and Moritz, C. (2011). Recent and rapid speciation with limited morphological disparity in the genus Rattus. *Syst. Biol.* 60, 188–203. doi: 10.1093/sysbio/syq092

Schaub, S. (1938). Tertiäre und quartäre Murinae. *Abh. Schweiz. Palaeontologischen Ges.* 61, 1–37.

Steppan, S. J., and Schenk, J. J. (2017). Muroid rodent phylogenetics: 900-species tree reveals increasing diversification rates. *PLoS One* 12:e0183070. doi: 10. 1371/journal.pone.0183070

Suzuki, H. (2020). "Evolutionary history of the subgenus *Mus* in Eurasia with special emphasis on the house mouse *Mus musculus*," in *Papers in Honour of Ken Aplin. Records Australian Mus*, Vol. 72, eds J. Louys, S. O'Connor, and K. M. Helgen (Darlinghurst NSW: Australian Museum) 317–323. doi: 10.3853/ j.2201-4349.72.2020.1727.

Tauxe, L., and Opdyke, N. D. (1982). A time framework based on magnetostratigraphy for the Siwalik sediments of the Khaur area, northern Pakistan. *Palaeogeogr. Palaeoclimatol. Palaeoecol.* 37, 43–61. doi: 10.1016/0031-0182(82)90057-8

Tedford, R. H., Qiu, Z.-x, and Flynn, L. J. (2013). "Late Cenozoic Yushe Basin, Shanxi Province, China: geology and fossil mammals," in *History, Geology, and Magnetostratigraphy*, Vol. I (Dordrecht: Springer).

Van Dam, J. A., Krijgsmann, W., Abels, H., Álvarez-Sierra, M. A., García-Paredes, I., López-Guerro, P., et al. (2014). Updated chronology for the middle to late Miocene mammal sites of the Daroca area (Calatayud-Mont Albán Basin, Spain). *Géobios* 47, 325–334. doi: 10.1016/j.geobios.2014.07.002